

Pozzolan activity of a spent fluid catalytic cracking catalyst residue

Pedro Garcés

Departamento Ingeniería de la Construcción, O. Públicas e Infraestructura Urbana, Universidad de Alicante, Spain

Fred P. Glasser

Department of Chemistry, University of Aberdeen, UK

Daniel R. M. Brew*

Department of Chemistry, University of Aberdeen, UK

Emilio Zornoza

Departamento de Ingeniería de la Construcción, Obras Públicas e Infraestructura Urbana, Universidad de Alicante, Spain

Jordi Payá

Instituto de Ciencia y Tecnología del Hormigón. Univ. Politécnica de Valencia, Spain

The reaction between a spent fluid cracking catalyst (FC3R) residue and portlandite was monitored over 56 days using several material characterisation techniques. The results showed that the residue was heterogeneous and composed of reactive and non-reactive fractions and that both fractions contained silicon and aluminium. After 56 days, the development of C–S–H gel was evident; part of the catalyst residue was pozzolan. The CH combination could be monitored by thermogravimetry or X-ray diffraction, by measuring the signal corresponding to CH. However, due to the low crystallinity of cementing products and their complex stoichiometry, the above-mentioned techniques were less able to characterise C–A–S–H. However, nuclear magnetic resonance techniques allowed the evolution of the pozzolan reaction to be evaluated and the hydrate products to be characterised.

Introduction

Spent fluid catalytic cracking catalyst (FC3R), recovered from petrol refineries, shows significant pozzolan activity in Portland cement and lime pastes (Hsu *et al.*, 2001; Pacewska *et al.*, 2002; Payá *et al.*, 1999, 2001, 2002, 2003a; Su *et al.*, 2000, 2001; Wu *et al.*, 2003). Although the source of FC3R may be different depending on the refinery, a previous study performed on five wasted catalysts coming from five different origins has shown that the source and the differing processing of the catalysts do not produce different behaviour, as the five studied materials presented a similar pozzolan reactivity (Payá *et al.*, 2009). One of the difficulties of introducing a novel pozzolan material into use is to ensure that the material has completely reacted with the cement or hydrated lime or, if the reaction is incomplete, it retains potential for further reaction. Due to the poor crystallinity of spent catalyst residues and the inherent challenges associated with their structural quantification, very little has been published on its reaction. Compressive strength development can, of course, indicate reaction as a function of time but the relationship between strength gain and reacted fraction does not provide an accurate description of the pozzolan activity of the spent catalyst.

In the present study, a spent catalyst residue, designated FC3R, has been reacted with calcium hydroxide so that the pozzolan

reaction can be monitored free of interference from supplementary cementitious materials and products, especially those containing iron. The pozzolan activity and course of reaction have been investigated using the following microstructural characterisation techniques: powder X-ray diffraction (XRD), Fourier transform infra-red spectroscopy (FT-IR) and ²⁷Al and ²⁹Si solid-state magic angle nuclear magnetic resonance spectroscopy (MAS NMR).

The special features of this study on FC3R relate both to the novel nature of the residue and to the use of calcium hydroxide as the activator, avoiding the presence of cementing materials from the cement hydration. In this manner the evolution of the simple pozzolan acid–base reaction (acid = pozzolan; base = CH) can be monitored without interference.

Experimental

The petrol refinery which supplied the spent FC3R residue was BP Oil España (Castellón, Spain). The reactivity of the catalyst was increased to the optimum particle size distribution with the aid of a laboratory ball mill (Gabbrielli Mill-2) (Payá *et al.*, 1999, 2001). In the preparation of the lime pastes, general purpose laboratory-grade (96% purity) calcium hydroxide (Pan-reac S.A., Spain) was used. The major oxide composition of spent FC3R, as supplied by the manufacturer, is given in Table 1. Table 2 shows the paste formulations that were prepared with the reagent proportions and the analyses that were performed for characterisation. The pastes were prepared to a uniform

* Current address: Institute of Materials Engineering, Australian Nuclear Science & Technology Organisation, Menai, New South Wales, Australia

Oxide	FC3R	Oxide	FC3R
SiO ₂	48.2	K ₂ O	< 0.01
CaO	< 0.01	SO ₃	0.04
Al ₂ O ₃	46.0	TiO ₂	1.65
Fe ₂ O ₃	0.95	Cl	< 0.01
MgO	< 0.01	LOI	1.50
Na ₂ O	0.50	IR	11.11

Table 1. Major oxide composition (in wt.%) of spent FC3R

water : cement weight ratio = 0.8 and cured at room temperature (22 ± 5°C) in sealed containers at ~100% relative humidity for the stated period of time. Prior to analysis, reaction was stopped by powdering the sample and quenching hydration by washing with acetone several times. The solid was filtered and dried at 60°C for 30 min in air.

A previous study (Payá *et al.*, 2001) reported that spent residues from this refinery were composed of a faujasite-like material. From XRD, the crystallinity of the spent catalyst had degraded relative to fresh material. Therefore, to help in interpreting the instrumental data on systems containing the FC3R residue, synthetic commercial faujasite, referred to as ‘faujasite’ in this study, was also used to benchmark FT-IR and MAS NMR studies. The FT-IR measurements were carried out using a Fourier transform infra-red spectrophotometer (Perkin Elmer; model 1740). The spectra were collected in the wavenumber range from 400 to 4000 cm⁻¹ and in an air atmosphere using the KBr pellet technique. Pellets were prepared by pressing a mixture of the sample and dried KBr (sample/KBr approximately 1 : 150) at 5 tonnes/cm². Powder XRD patterns were collected using a Bruker D8 Advance diffractometer with twin Gobel mirrors using CuK_α radiation. Data were collected over the range 5 < 2θ < 60° with a step size of 0.02°. The NMR spectra were performed by a Varian UNITY Inova 7.5 mm MAS probe spectrometer with a 7.05 T (‘300 MHz’) Oxford Instruments magnet. Samples were spun in zirconia rotors at a maximum of 7 kHz. Sufficient scans of nuclei were collected to minimise signal degradation. Where appropriate, samples were cross-polarised using a contact time of 10 ms. Cross-polarisation can be used when investigating very dilute nuclei and/or less mobile

nuclei which are fixed in rigid structures such as ²⁹Si in cements or silicate minerals. The technique can determine which nuclei are in close vicinity to hydrogens – in the present study hydrogens would be present as hydroxyl groups. The ²⁹Si and ²⁷Al nuclei under observation were referenced to the standards: tetramethyl silane and 1 mol/l AlCl₃, respectively.

Results

Figure 1 illustrates the XRD pattern of spent FC3R catalyst residue. The residue contains both semi-crystalline and crystalline material. The broad hump feature at 2θ values between 20 and 30° indicates the presence of semi-crystalline or amorphous material, as does the low signal : noise ratio of the pattern. Reflections pertaining to the mineral faujasite, Na₂O·Al₂O₃·4.7SiO₂·xH₂O (JCPDS file 39-1380) were identified. Minor reflections can be attributed to cristobalite (JCPDS file 76-0939), mullite (JCPDS file 73-1253) and quartz (JCPDS file 46-1045). These phases have been reported previously in XRD analyses of other spent commercial faujasite-based catalysts (Chen *et al.*, 2004, Payá *et al.*, 2001).

Figure 2 illustrates the XRD pattern obtained for sample FC3R0 (t = 0 days: within about 15 min after mixing). All major reflections correspond to portlandite (Ca(OH)₂; JCPDS file

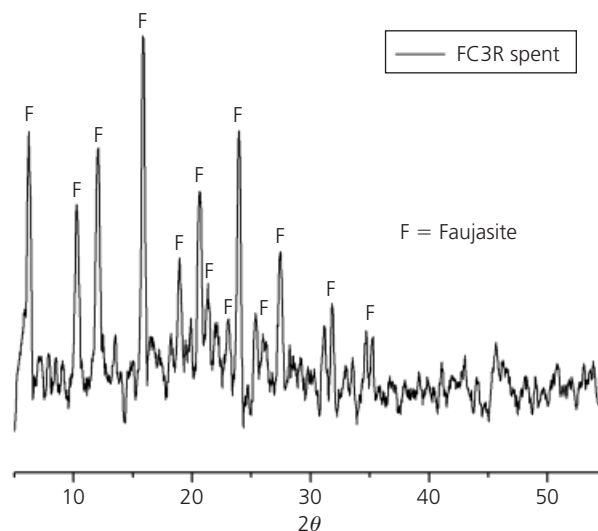


Figure 1. Powder XRD pattern for spent FC3R residue

Sample	Description (ratio)	Cure: days	XRD	FT-IR	NMR
FC3R0	FC3R/CH (3/7)	0	✓		✓
FC3R1	FC3R/CH (3/7)	1		✓	
FC3R3	FC3R/CH (3/7)	3	✓		✓
FC3R7	FC3R/CH (3/7)	7		✓	
FC3R28	FC3R/CH (3/7)	28	✓	✓	✓
FC3R56	FC3R/CH (3/7)	56			✓

Table 2. Formulations of pastes and instrumental analyses made

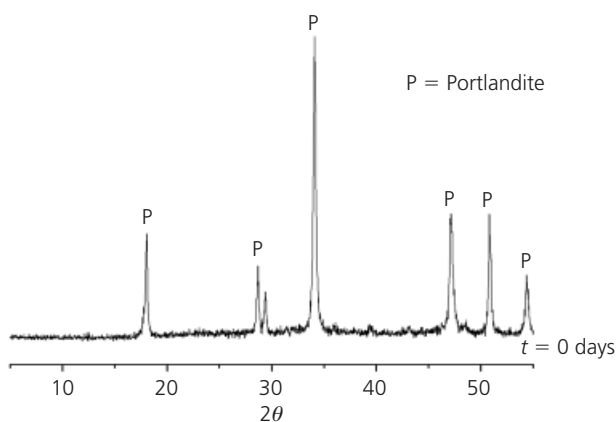


Figure 2. XRD pattern for FC3R0 paste

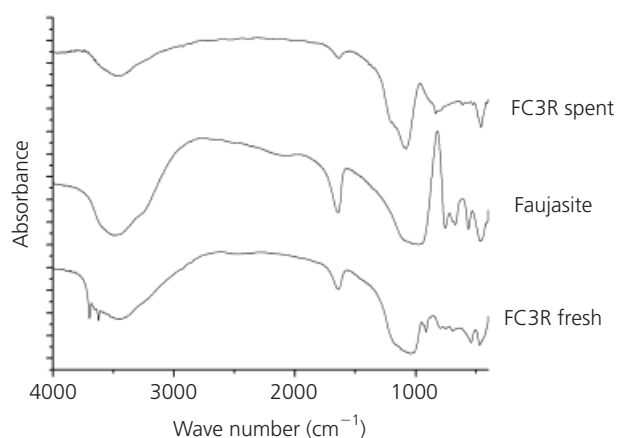


Figure 4. FT-IR spectra of spent and fresh FC3R and synthetic faujasite

04-793). Comparison of the XRD patterns obtained in Figures 1 and 2 shows that, in the latter case, peaks attributed to faujasite have apparently disappeared due to the highly crystalline nature of portlandite and the relatively low faujasite content. Figure 3 collates the XRD patterns of FC3R0, FC3R3 and FC3R28. In each case the major reflections also correspond to portlandite. The continued presence of $\text{Ca}(\text{OH})_2$ as a function of time can be clearly observed although it is evident that the intensity of the characteristic reflections diminish as the reaction time increases. At the same time, new reflections appear. The reflection situated near 2θ value of 12° indicates the possible development of stratlingite, $\text{Ca}_2\text{Al}_2(\text{SiO}_2)(\text{OH})_{10}\cdot 2.5\text{H}_2\text{O}$ (JCPDS file 29-0285). This reflection strengthens as curing time increases.

Figure 4 presents the FT-IR spectra of faujasite, spent FC3R residue and fresh FC3R catalyst. In general the spectra for all three materials show some similarities. However, there are two main differences between spent and fresh FC3R. First, fresh FC3R gives rise to H-bonding absorptions located approximately

at 3750 cm^{-1} indicative of molecular water. The conversion process, from fresh catalyst to spent FC3R residue, occurs under the influence of heat as well as chemical impurities and, as a result, these vibrations are absent. Second the silicate and aluminosilicate framework vibrations present in the spent residue, from about $1100\text{--}470\text{ cm}^{-1}$ and below, appear less well developed and have shifted slightly suggesting that the spent catalyst has a different network structure than fresh material. The spent residue also gives rise to a OH stretching and a deformation vibration at $3000\text{--}3500$ and 1640 cm^{-1} , respectively. Table 3 collates the principal wavenumbers and their assignments which agree well with studies previously reported (Pacewska *et al.*, 2000, Payá *et al.*, 2003b).

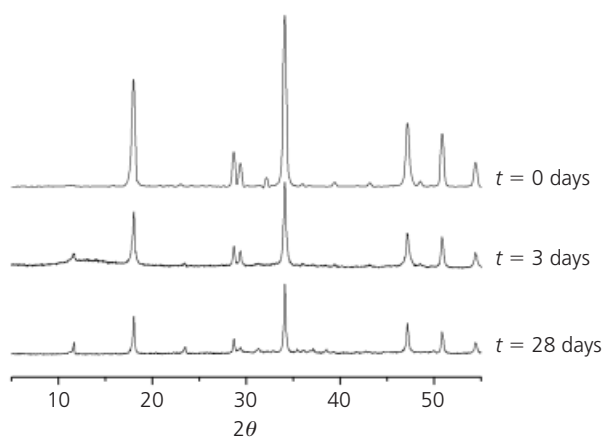


Figure 3. XRD patterns for FC3R0, 3 and 28 as a function of curing time

Figure 5 presents the FT-IR spectra for mixtures of $\text{Ca}(\text{OH})_2$, FC3R1, FC3R7 and FC3R28. It can be seen that vibrations for $\text{Ca}(\text{OH})_2$ are present in all three FC3R spectra. There is little spectral difference between FC3R1 and FC3R7 (1 and 7 days hydration time) but after 28 days, significant pozzolanic reaction has occurred, as indicated by both the reduction in intensity of the sharp vibration at 3640 cm^{-1} , assigned to hydroxide stretching from $\text{Ca}(\text{OH})_2$, and the broader hydroxide deformation absorption near 1500 cm^{-1} .

Vibration (cm^{-1})	Assignment
3000–3500	OH stretching H_2O
1640	OH deformation
1150	Si–O stretching
1070	Si–O(Al) stretching
800	Si–O tetrahedra stretching
550	Si–OH stretching
470	Si–O–Si deformation

Table 3. FT-IR data for spent FC3R residue

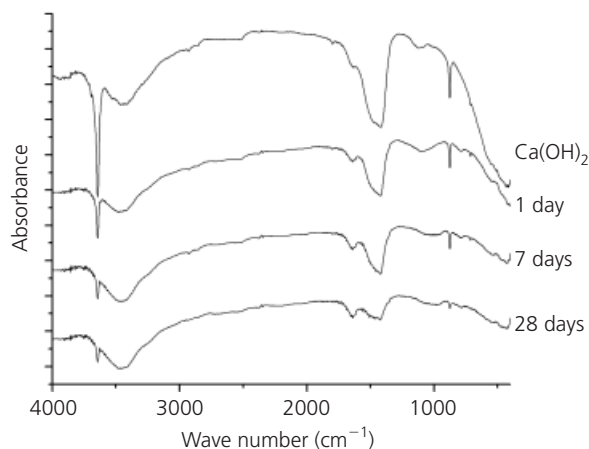


Figure 5. FT-IR spectra of Ca(OH)₂, FC3R1, FC3R7 and FC3R28

The ²⁹Si, {¹H-²⁹Si} CP and ²⁷Al MAS NMR spectra of spent FC3R residue are displayed in Figure 6. The spectra confirm that the spent residue was a heterogeneous mixture containing both crystalline and semi-crystalline phases. The sharp peak observed at -108.4 ppm suggests an ordered Q⁴ silicate phase, probably quartz and/or cristobalite, known from XRD to be present. A range of Q², Q³ and Q⁴ Si-O(Al) environments are scattered between -115 to -80 ppm. The ²⁷Al MAS NMR spectrum shows both broad and sharp peaks can be observed, indicative of a spread of Al-O environments. The sharpest peak observed at 5.5 ppm is partly obscured by broader peaks but arises from the presence of octahedrally-coordinated aluminium. The broader

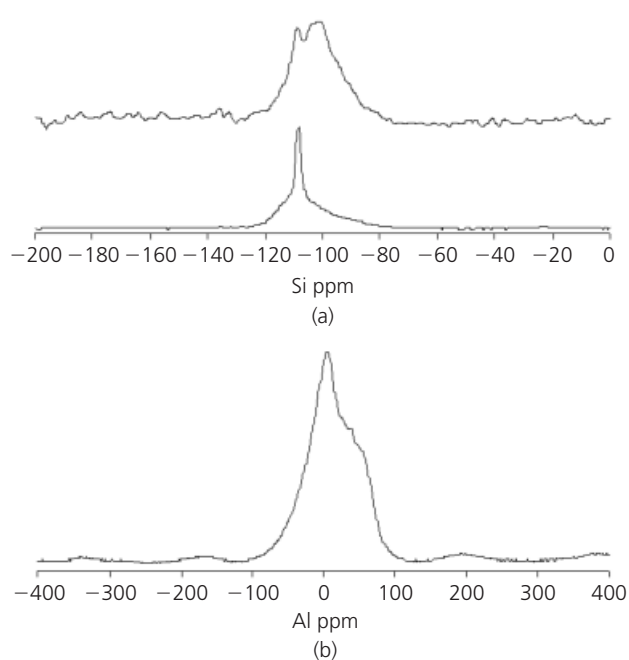


Figure 6. ²⁹Si ((a), lower) and {¹H-²⁹Si} CP ((a), upper) and ²⁷Al MAS NMR (b) spectra of spent FC3R residue

peaks, located near 35 and 55 ppm, are characteristic of pentahedral and tetrahedral aluminium, respectively. The other feature of this spectrum, bands at -400, -200, 200 and 400 ppm, are attributed to spinning sidebands. These are artefacts due to the presence of trace quadrupolar nuclei, such as iron, sodium, etc. and, while they should be discounted as signal due to Al, they serve to further highlight the heterogeneity of the residue. Figure 7 presents the ²⁹Si, {¹H-²⁹Si} CP and ²⁷Al MAS NMR spectra of faujasite. Five different Si-O environments are associated with the material at -84.6, -89.0, -93.7, -98.3 and -102.2 ppm and all have hydroxyls in close vicinity, indicating a homogeneous material. The most abundant shift at -84.6 ppm corresponds to a single type of Q² Si (chain silicates). The shift at -89.0, while also in the Q² range, is more likely to be a Q³(2Al) or Q³(3Al) environment: chain-branching Si-O with two or three aluminium atoms close by; the aluminium nuclei interfere with the silicon nuclei response to the applied magnetic field resulting in a lower chemical shift than expected. The resonances at -93.7, -98.3 and -102.2 ppm are Q³ chain-branching Si-O without aluminium nuclei as next-to-nearest neighbours. In addition, Figure 7 shows a sharp ²⁷Al shift at -59.8 ppm indicative of a singular tetrahedrally-coordinated Al-O environment.

Figure 8 presents the ²⁹Si, {¹H-²⁹Si} CP and ²⁷Al MAS NMR spectra of FC3R3. First, the ²⁹Si MAS NMR spectrum has a low signal : noise ratio despite the large number of scans collected. This would suggest a poorly-ordered system that is composed of Q¹, Q², Q³ and Q⁴ siliceous environments. The cross-polarised

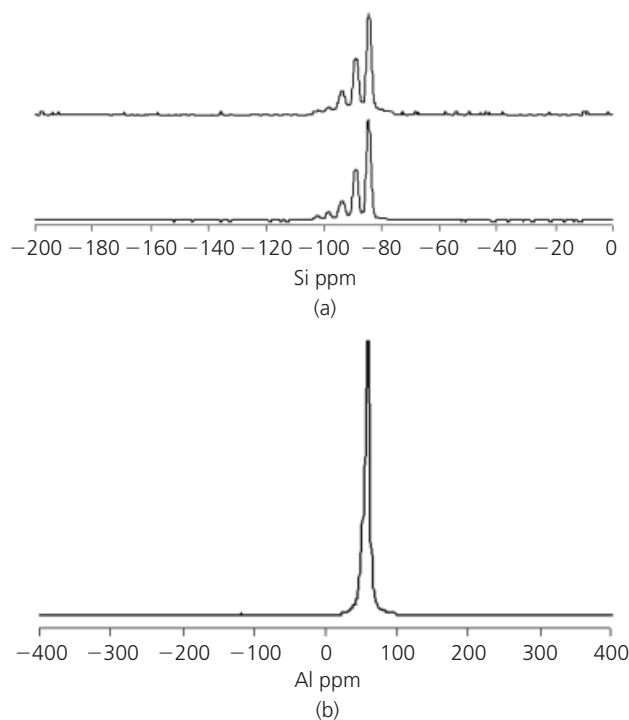


Figure 7. ²⁹Si MAS ((a), lower), {¹H-²⁹Si} CP ((a), upper) and ²⁷Al MAS NMR (b) spectra of synthetic faujasite

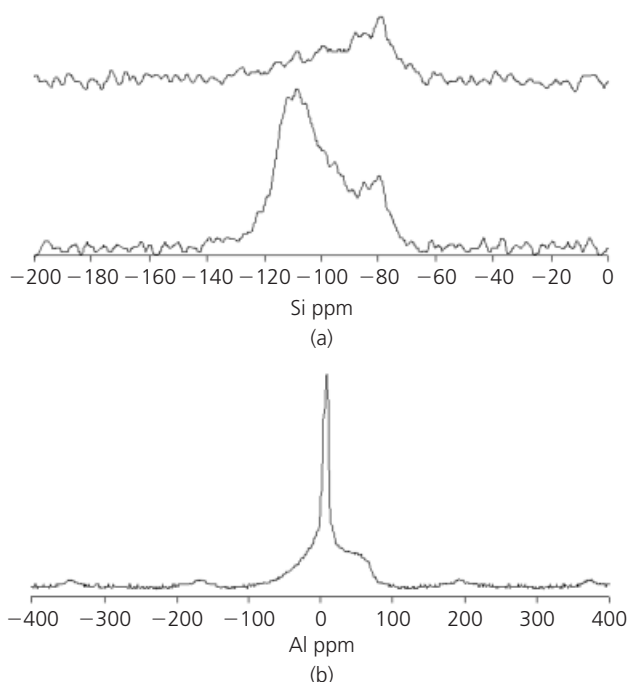


Figure 8. ^{29}Si MAS ((a), lower), $\{^1\text{H-}^{29}\text{Si}\}$ CP ((a), upper) and ^{27}Al MAS NMR (b) spectra of FC3R3

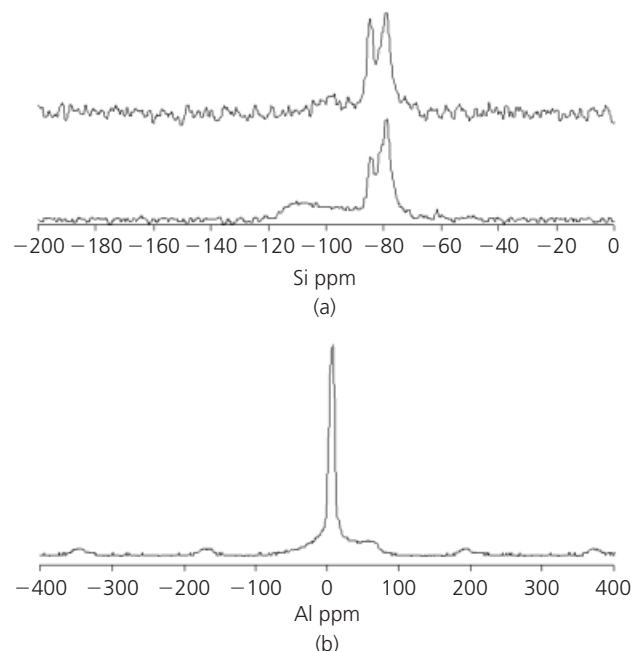


Figure 9. ^{29}Si MAS ((a), lower), $\{^1\text{H-}^{29}\text{Si}\}$ CP ((a), upper) and ^{27}Al MAS NMR (b) spectra of FC3R28

spectrum shows that hydroxyls are predominantly associated with the Q^1 and Q^2 environments – consistent with early formation of C–S–H gel – with minor amounts near the Q^3 and Q^4 Si–O environments. The ^{27}Al MAS spectrum reveals that only some of the aluminium is reactive in spent FC3R residue; that is, all of the pentahedral and some of the tetrahedral aluminium has reacted. The octahedral aluminium appeared unchanged in its chemical shift but still might have been incorporated into the C–S–H gel as reported previously (Sun *et al.*, 2006). The unreactive aluminous fraction was composed of tetrahedral and possibly octahedral aluminium.

Figure 9 presents the ^{29}Si , $\{^1\text{H-}^{29}\text{Si}\}$ CP and ^{27}Al MAS NMR spectra of FC3R28. It can be seen that the ^{29}Si and CP MAS spectra are very different from those of FC3R3, suggesting considerable reaction has taken place. In general, most of the Q^3 Si–O environments have been consumed to yield relatively sharp Q^1 and Q^2 Si–O environments, inferring improved local order at -79 and -84 ppm, respectively. There is evidence of minor persistent siliceous material in the Q^4 spectral region. It is noteworthy that the peak at -108 ppm, present in the FC3R residue starting material, has vanished suggesting its consumption has occurred. From the $\{^1\text{H-}^{29}\text{Si}\}$ CP MAS NMR spectrum, the hydroxyls are associated with the Si–O phases in the Q^1 and Q^2 regions. The ^{27}Al MAS NMR spectrum shows the Al–O environment is predominantly octahedral with minor residual tetrahedral aluminium. This is interpreted as indicating that some aluminium within the FC3R residue is reactive and some is not. Figure 10 presents the ^{29}Si , $\{^1\text{H-}^{29}\text{Si}\}$ CP and ^{27}Al MAS NMR spectra of

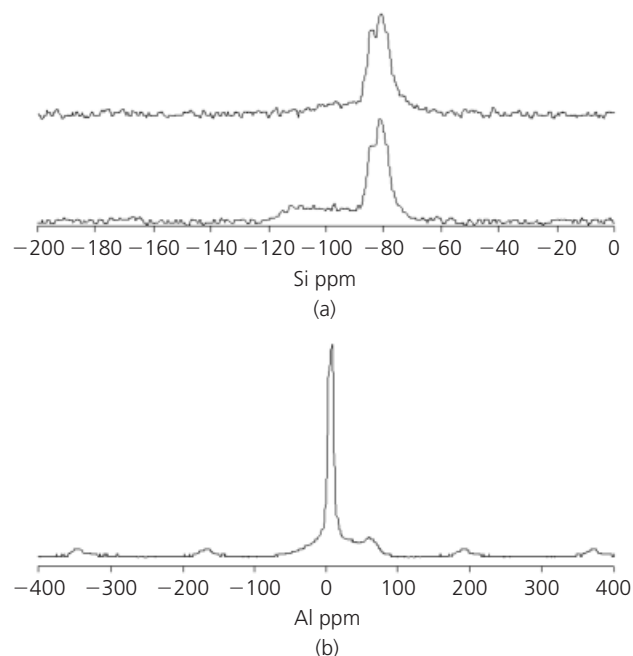


Figure 10. ^{29}Si MAS ((a), lower), $\{^1\text{H-}^{29}\text{Si}\}$ CP ((a), upper) and ^{27}Al MAS NMR (b) spectra of FC3R56

FC3R56. The ^{29}Si spectra show that the silicate microstructure has continued to develop – most of the Q^1 Si–O environments have polymerised to yield two distinct Q^2 (located at -81 and -84 ppm) environments with minor amounts of siliceous Q^4 material persisting. However, the hydroxyls are associated with

the Q^2 silicon nuclei and not with those of Q^4 . The ^{27}Al MAS NMR spectrum has not changed significantly from 28 to 56 days reaction time, with most aluminium being octahedrally coordinated with minor tetrahedral.

Discussion

The acceptance of novel pozzolanic materials is a slow process. To speed the acceptance process, spent FC3R catalyst residue was reacted with $\text{Ca}(\text{OH})_2$ to quantify its pozzolanic reactivity. XRD and NMR data showed that the as-received residue contained both crystalline and semi-crystalline material. The latter is both siliceous and aluminous and has hydroxyl groups in close proximity. After 3 days, the ^{29}Si and $\{^1\text{H}-^{29}\text{Si}\}$ MAS NMR spectra show that the reaction product(s) has a range of Q^2 , Q^3 and Q^4 Si–O(Al) environments with resonances between -115 to -80 ppm. Partial pozzolanic reaction is also evidenced by the cross-polarised spectrum: hydroxyls are associated with the Q^2 silicon environments, indicative of C–S–H gel, albeit silicon-poor. However, the large, broad Q^3 peaks in both the ^{29}Si and $\{^1\text{H}-^{29}\text{Si}\}$ CP spectra suggested that significant FC3R residue remained unreacted after only 3 days. With respect to aluminium, all of the pentahedral and the majority of tetrahedral fractions were consumed within the first 3 days of reaction, leaving a residue material containing octahedral and a minor quantity of tetrahedral aluminium. The remaining octahedrally-coordinated aluminium appeared to be part of a crystalline phase due to its sharpness – possibly stratlingite-like, as suggested by XRD, although stratlingite contains both tetrahedral and octahedral aluminium.

The pozzolanic reaction continued with time. After 28 days, diminution of reflection and vibration intensities were observed in the XRD patterns and FT-IR spectra presented in Figures 3 and 5, respectively. The diminution was due to reaction between FC3R and $\text{Ca}(\text{OH})_2$ and the NMR evidence shows that during this reaction, much of the Q^3 Si–O environments were consumed to yield Q^1 and Q^2 Si–O environments. These were typically observed in the Q^1 and Q^2 region of the spectrum and assigned to C–S–H gel. From the $\{^1\text{H}-^{29}\text{Si}\}$ CP MAS NMR spectrum in Figure 9, hydroxyls were associated with the Si–O phases in the Q^1 or Q^2 (Al) region, in accordance with other evidence corroborating the formation of a C–S–H gel or C–A–S–H gel, or both. Poorly-ordered Q^4 siliceous material still persisted and ^{27}Al MAS NMR evidence showed that not all of the tetrahedral aluminium had reacted within 28 days. After 56 days, the two separate Q^1 and Q^2 silicon regions continued to develop into characteristic C–S–H gel resonances. The persistence of Q^4 siliceous and tetrahedral aluminous material infers that not all the spent residue is reactive and that some of the silicon and aluminium will not contribute to formation of cementitious bonds within 56 days.

Therefore, spent catalysts seem to offer a potential use as pozzolanic material to be incorporated in mortars and concrete. In fact, other authors have reported good mechanical and

durability properties when they have been used as cement replacement. This residue has been mechanically tested to show a proper compatibility with several types of cements (Zornoza *et al.*, 2007). With regard to durability aspects, the protection that blended cements incorporating FC3R offer to steel reinforcements is similar or better than plain Portland cement mortars when a carbonation or chloride-induced attack is considered (Zornoza *et al.*, 2008, 2009). The resistance to sulfates of mortars has also been improved by the incorporation of spent catalyst in mix formulations by reducing the strength decrease that experimented plain cement mortars (Bukowska *et al.*, 2003). However, one factor that should be considered is the maximum quantity of this pozzolan that can be used to obtain an optimal performance, which most authors limit to 15 to 20% of cement weight.

Conclusion

The following conclusions can be drawn from the results from the present study.

- XRD, FT-IR and NMR data demonstrate the pozzolanic activity of FC3R when mixed with $\text{Ca}(\text{OH})_2$ pastes.
- According to ^{29}Si and ^{27}Al MAS NMR data, the pozzolanic reaction of spent catalyst yields mainly linear chains of silicates with possible incorporation of predominantly octahedral aluminium. On the basis of the results obtained, solid-state NMR was the most suitable technique to monitor the development of the pozzolanic reaction.
- A fraction of FC3R – composed of Q^4 siliceous material and tetrahedral aluminium – did not react and persisted even after 56 days hydration.
- Spent faujasite catalyst shows promise as a potential pozzolanic material. Products of reaction with $\text{Ca}(\text{OH})_2$ include C–A–S–H and an AFm phase, probably stratlingite-like.

REFERENCES

- Bukowska M, Pacewska B and Wilinska I (2003) Corrosion resistance of cement mortars containing spent catalyst of fluidized bed cracking (FBCC) as an additive. *Journal of Thermal Analysis and Calorimetry* **74**(3): 931–942.
- Chen H-L, Tseng Y-S and Hsu K-C (2004) Spent FCC catalyst as a pozzolanic material for high-performance mortars. *Cement and Concrete Composites* **26**(6): 657–664.
- Hsu K-C, Tseng Y-S, Ku F-F and Su N (2001) Oil cracking waste catalyst as an active pozzolanic material for superplasticized mortars. *Cement and Concrete Research* **31**(12): 1815–1820.
- Pacewska B, Wilinska I and Bukowska M (2000) Hydration of cement slurry in the presence of spent cracking catalyst. *Journal of Thermal Analysis and Calorimetry* **60**(1): 71–78.
- Pacewska B, Bukowska M, Wilinska, I and Swat M (2002) Modification of the properties of concrete by a new pozzolan. A waste catalyst from the catalytic process in a fluidized bed. *Cement and Concrete Research* **32**(1): 145–152.
- Payá J, Monzó J and Borrachero MV (1999) Fluid catalytic cracking catalyst residue (FCC). An excellent mineral by-product for improving early-strength development of cement

- mixtures. *Cement and Concrete Research* **29(11)**: 1773–1779.
- Payá J, Monzó J and Borrachero MV (2001) Physical, chemical and mechanical properties of fluid catalytic cracking catalyst residue (FCC) blended cements. *Cement and Concrete Research* **31(1)**: 57–61.
- Payá J, Monzó J, Borrachero MV, et al. (2002) Advantages in the use of fly ashes in cements containing pozzolanic combustion residues: silica fume, sewage sludge ash, spent fluidized bed catalyst and rice husk ash. *Journal of Chemical Technology and Biotechnology* **77(3)**: 331–335.
- Payá J, Monzó J, Borrachero MV and Velázquez S (2003a) Evaluation of the pozzolanic activity of fluid catalytic cracking residue (FCC). Thermogravimetric analysis studies on FCC-Portland cement pastes. *Cement and Concrete Research* **33(4)**: 603–609.
- Payá J, Monzó J, Borrachero MV, Velázquez S and Bonilla M (2003b) Determination of the pozzolanic activity of fluid catalytic cracking residue. Thermogravimetric analysis studies on FC3R-lime pastes. *Cement and Concrete Research* **33(7)**: 1085–1091.
- Payá J, Borrachero MV, Monzo J and Soriano L (2009) Studies on the behaviour of different spent fluidized-bed catalytic cracking catalysts on Portland cement. *Materiales de Construcción* **59(296)**: 39–54.
- Su N, Fang H-Y, Chen Z-H and Lu F-S (2000) Reuse of waste catalysts from petrochemical industries for cement substitution. *Cement and Concrete Research* **30(11)**: 11, 1773–1783.
- Su N, Chen Z-H and Fang H-Y (2001) Reuse of spent catalyst as fine aggregate in cement mortar. *Cement and Concrete Composites* **23(1)**: 111–118.
- Sun GK, Young F and Kirkpatrick RJ (2006) The role of Al in C–S–H: NMR, XRD and compositional results for precipitated samples. *Cement and Concrete Research* **36(1)**: 18–29.
- Wu J-H, Wu W-L and Hsu K-C (2003) The effect of waste oil-cracking catalyst on the compressive strength of cement pastes and mortars. *Cement and Concrete Research* **33(2)**: 245–253.
- Zornoza E, Garcés P, Monzó J, Borrachero MV and Payá J (2007) Compatibility of fluid catalytic cracking catalyst residue (FC3R) with various types of cement. *Advances in Cement Research* **19(3)**: 117–124.
- Zornoza E, Garcés P and Payá J (2008) Corrosion rate of steel embedded in blended Portland and fluid catalytic cracking catalyst residue (FC3R) cement mortars. *Materiales de Construcción* **58(292)**: 27–43.
- Zornoza E, Garcés P, Payá J and Climent MA (2009) Improvement of the chloride ingress resistance of OPC mortars by using spent cracking catalyst. *Cement and Concrete Research* **39(2)**: 126–139.

WHAT DO YOU THINK?

To discuss this paper, please submit up to 500 words to the editor at www.editorialmanager.com/acr by 1 October 2011. Your contribution will be forwarded to the author(s) for a reply and, if considered appropriate by the editorial panel, will be published as a discussion in a future issue of the journal.